

1 **Supplemental material**

2

3 Eq. S1: $\frac{[CH_4]_{av.west} - [CH_4]_{av.east}}{[CH_4]_{av.west} + [CH_4]_{av.east}} * 100 (\%)$

4

5 Table S1: All seawater methane samples collected for measuring the dissolved methane concentrations and
 6 the potential oxidation rates. Here we show all the samples collected, including the duplicated samples
 7 (28x2 experimental and 76 discrete).

8

Stations	Depth (m)	Date collection	In-situ samples	Methane incubations
3	609	7/20/2019	x	x
3	419	7/20/2019	x	
3	310	7/20/2019	x	
3	151	7/20/2019	x	
3	71	7/20/2019	x	
3	40	7/20/2019	x	
3	7	7/20/2019	x	x
5	745	7/22/2019	x	x
5	601	7/22/2019	x	
5	455	7/22/2019	x	
5	381	7/22/2019	x	
5	175	7/22/2019	x	
5	21	7/22/2019	x	x
5	1	7/22/2019	x	x
8	561	7/23/2019	x	
8	451	7/23/2019	x	x
8	390	7/23/2019	x	
8	210	7/23/2019	x	
8	101	7/23/2019	x	
8	70	7/23/2019	x	x
8	15	7/23/2019	x	x
8	1	7/23/2019	x	
16	690	7/24/2019	x	x
16	502	7/24/2019	x	x
16	378	7/24/2019	x	
16	202	7/24/2019	x	
16	101	7/24/2019	x	
16	65	7/24/2019	x	
16	30	7/24/2019	x	
16	1	7/24/2019	x	x
20	144	7/26/2019	x	x
20	110	7/26/2019	x	
20	81	7/26/2019	x	
20	50	7/26/2019	x	

20	28	7/26/2019	x	x
20	19	7/26/2019	x	
20	2	7/26/2019	x	
21	136	7/26/2019	x	x
21	75	7/26/2019	x	
21	45	7/26/2019	x	
21	15	7/26/2019	x	
21	10	7/26/2019	x	x
23	181	7/28/2019	x	x
23	101	7/28/2019	x	
23	26	7/28/2019	x	
23	5	7/28/2019	x	x
26	208	7/29/2019	x	x
26	150	7/29/2019	x	
26	100	7/29/2019	x	
26	75	7/29/2019	x	
26	25	7/29/2019		x
26	1	7/29/2019	x	
30	251	7/30/2019	x	x
30	151	7/30/2019	x	
30	76	7/30/2019	x	
30	28	7/30/2019	x	x
30	2	7/30/2019	x	
31	207	7/30/2019	x	x
31	131	7/30/2019	x	
31	61	7/30/2019	x	
31	36	7/30/2019	x	x
31	2	7/30/2019	x	
41	380	8/1/2019	x	x
41	316	8/1/2019	x	
41	200	8/1/2019	x	
41	173	8/1/2019	x	
41	90	8/1/2019	x	
41	45	8/1/2019	x	
41	25	8/1/2019	x	x
41	1	8/1/2019	x	
52	241	8/4/2019	x	x
52	200	8/4/2019	x	
52	76	8/4/2019	x	
52	30	8/4/2019	x	
52	10	8/4/2019	x	
52	7	8/4/2019	x	x
52	2	8/4/2019	x	

10 Table S2: Dissolved in-situ methane in sea ice. In the table below we showed the sample ID, the vertical
 11 horizon along the core length, the temperature of sea ice, the methane isotopic signature, and the methane
 12 concentration. The sea ice salinity data were generated by the University of Illinois at Chicago and are
 13 publicly available at <https://doi.pangaea.de/10.1594/PANGAEA.937543>.

14

Sea Ice ID	Depth (cm)	Temperature (°C)	$\delta^{13}\text{CH}_4$ (‰)	[CH ₄] (nM)
1	10	2.1	-35.39	3.40
1	52	1.7	-46.38	21.25
1	82	1.4	-47.79	8.49
1	117	1.3	-39.77	8.32
1	190	1.2	-46.64	17.06
2	20	2	-42.00	8.01
2	50	1.2	-45.04	8.46
2	70	1.2	-47.24	6.25
2	90	1.6	-41.61	7.76
2	100	1.7	-39.49	4.11
3	10	1.8	-42.79	10.32
3	30	1.3	-47.20	6.95
3	60	0.9	-51.38	6.30
3	90	0.8	-45.53	11.66
4	20	1.4	-40.15	6.54
4	30	0.9	-38.65	5.96
4	90	0.4	-37.35	5.63
4	130	0.1	-40.78	7.33
4	146	0.1	-42.66	6.34
5	10	0.4	-38.65	5.97
5	20	0.5	-44.07	18.99
5	50	0.9	-40.42	6.15
5	70	1.2	-47.65	20.78
5	91	1.3	-36.73	8.23

15

16

17 Table S3: Incubation time of experimental samples collected at each CTD station.

18

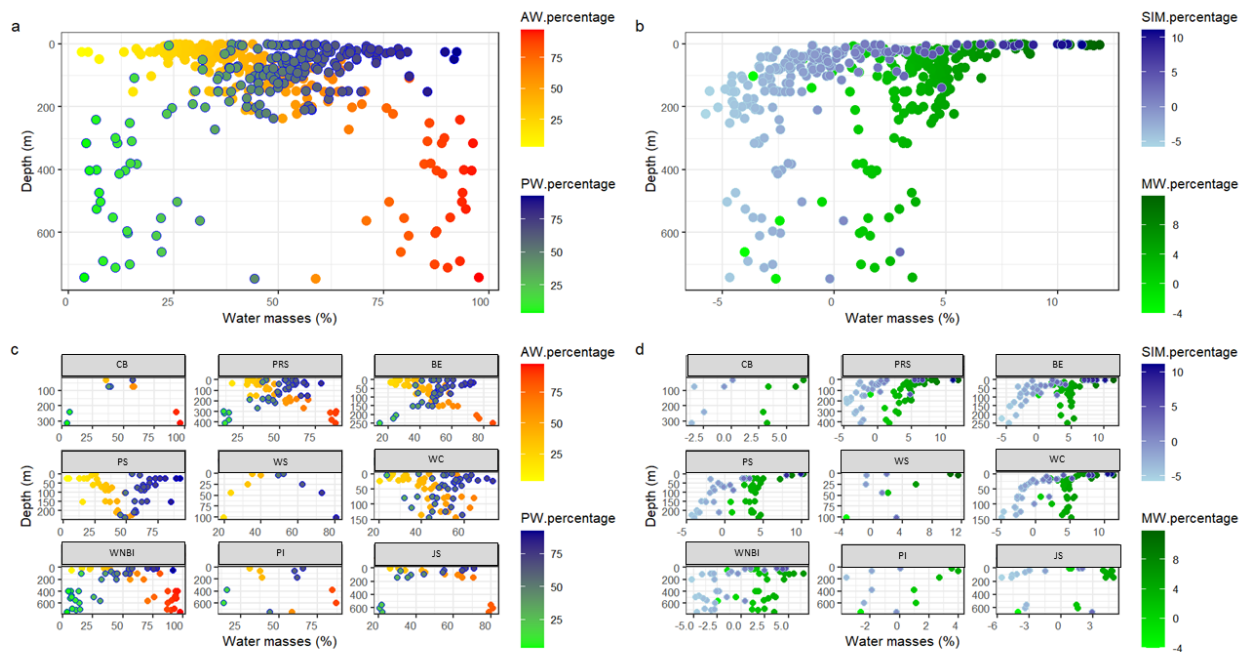
CTD station	Days of incubation
Jones Sound	24
West Navy Board Inlet	19
Wellington Channel	5
Prince Regent Sound	12
Croker Bay	7

19

20 Table S4: Information on experimental samples is presented in the table below, including the sampling
 21 location and depth, collection date, and volume of methane standard injected into each sample for oxidation
 22 rate measurement.

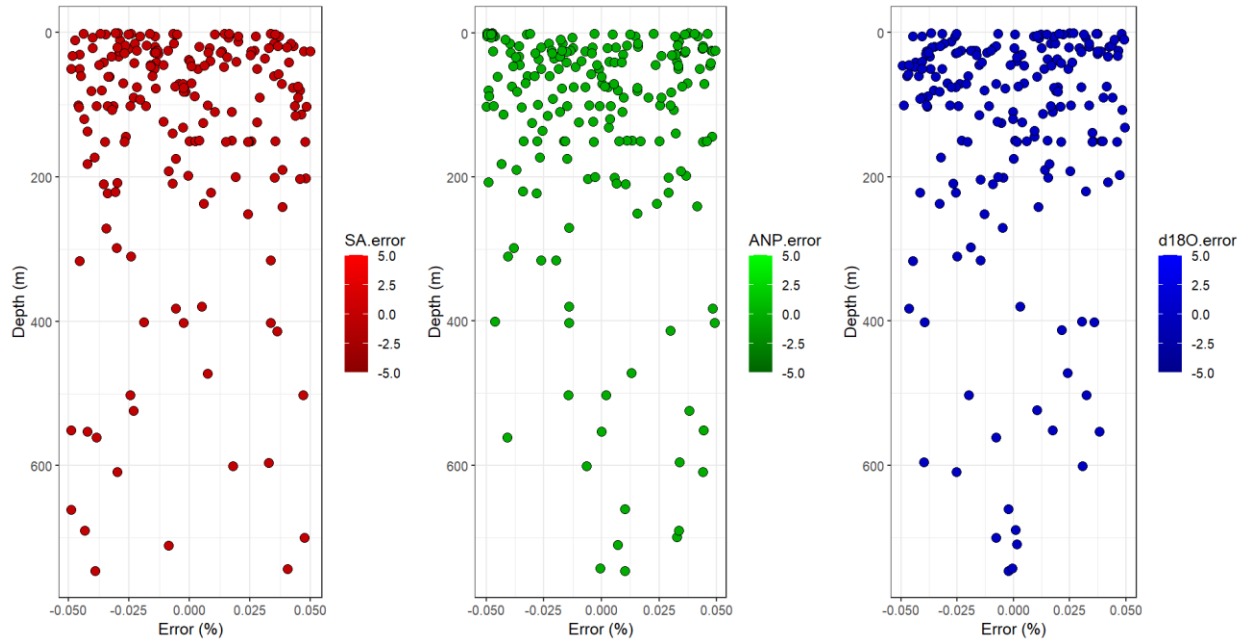
CTD station	Date	Depth (m)	CH ₄ spike (ml)
Jones Sound	7/19/2019	609	1
Jones Sound	7/19/2019	7	1
West of Navy Board Inlet	7/23/2019	70	2.5
West of Navy Board Inlet	7/23/2019	15	2.5
West of Navy Board Inlet	7/23/2019	450	2.5
West of Navy Board Inlet	7/23/2019	70	2.5
West of Navy Board Inlet	7/24/2019	743	2.5
West of Navy Board Inlet	7/24/2019	401	2.5
Wellington Channel	7/26/2019	10	2.5
Prince Regent Sound	7/31/2019	25	2.5
Croker Bay	8/3/2019	7	2.5
Croker Bay	8/3/2019	241	2.5

24
25
26



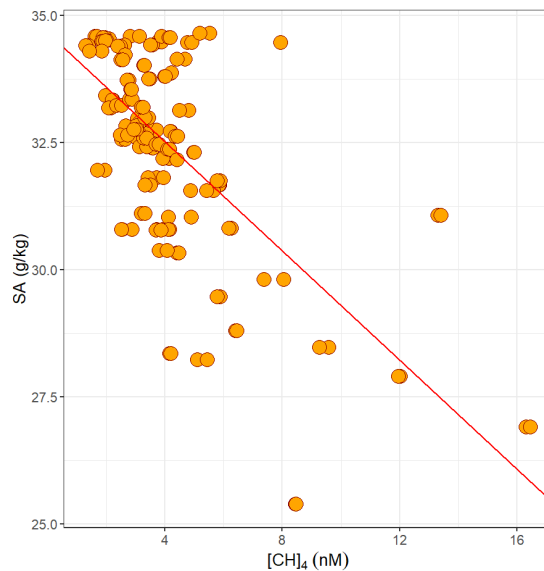
27
28
29
30
31
32
33
34
35

Figure S1: Profiles of water mass fractions across depth. Figure S1a depicts the distribution of water mass fractions, specifically the percentages of Atlantic Waters (AW) and Pacific Waters (PW). In Figure S1b, the contribution of meltwater, encompassing meteoric meltwater (MW) and sea ice meltwaters (SIM), is presented as percentages. Figure S1c displays the percentages of AW and PW at each station. Finally, Figure S1d illustrates the percentages of MW and SIM at each station. These profiles provide valuable insights into the variations and contributions of different water masses throughout the depth profile. The headers represent the sampling station as described in Fig. 1.



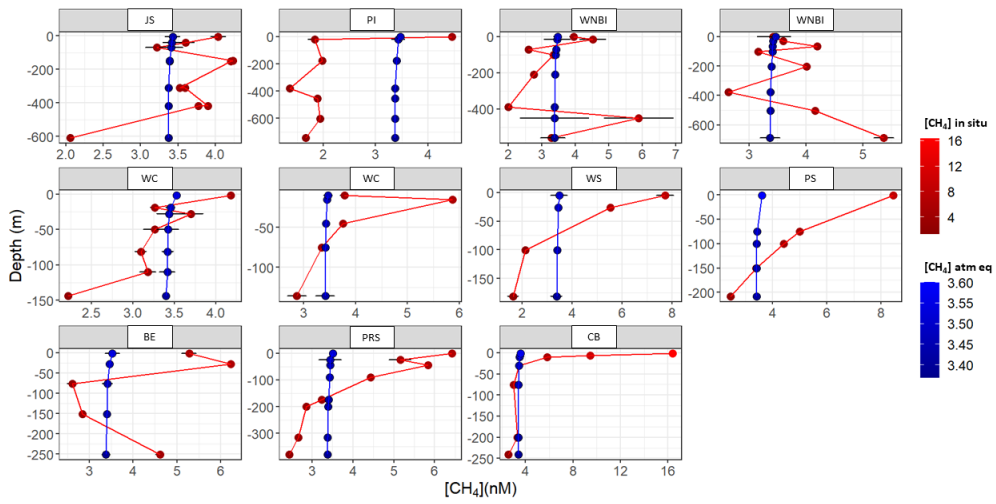
36
 37 Figure S2: The graph illustrates calculated errors for each endmember in the basic 4-endmember mass
 38 balance. It highlights mass fractions with deviations exceeding 5% from the expected value of 1, signifying
 39 notable discrepancies. Remarkably, all data points on the graph fall within a narrow range (-0.05% to
 40 0.05%), indicating a favorable level of uncertainty. The SA endmember is denoted by the red color code,
 41 ANP by the green color, and $\delta^{18}\text{O}$ by the blue color.

42



43
 44 Figure S3: Scatterplot of the in-situ methane concentration $[\text{CH}_4]$ and absolute salinity (SA) with a robust
 45 linear regression line. The abline to the plot is based on the intercept and slope estimates from the robust
 46 linear regression model. (R^2 : 0.4223, p-value: $< 2.2\text{e-}16$).

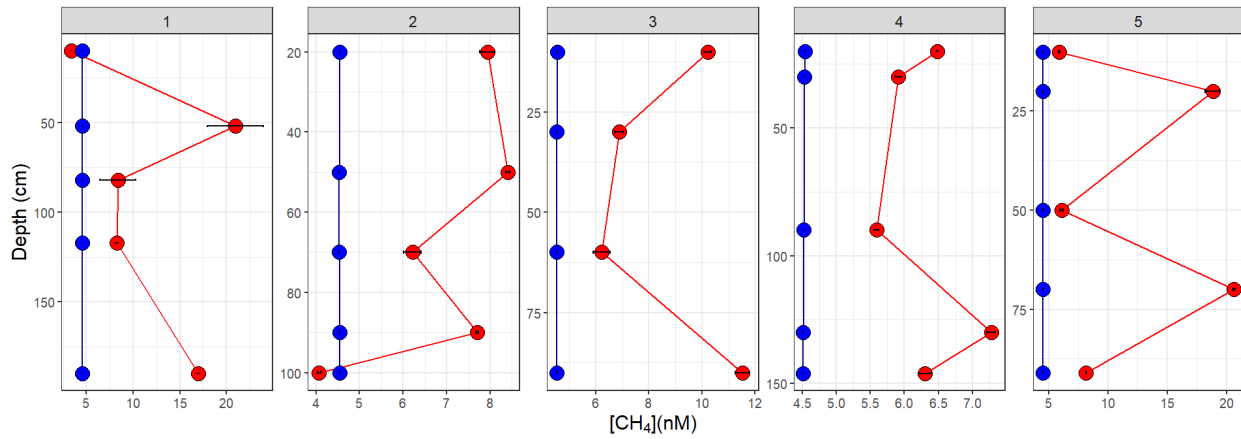
47



48

49 Figure S4: All methane vertical profiles. In red are the in-situ $[CH_4]$, while in blue are the $[CH_4]$ at
 50 atmospheric equilibrium. The headers show the CTD stations as described in Fig.1.

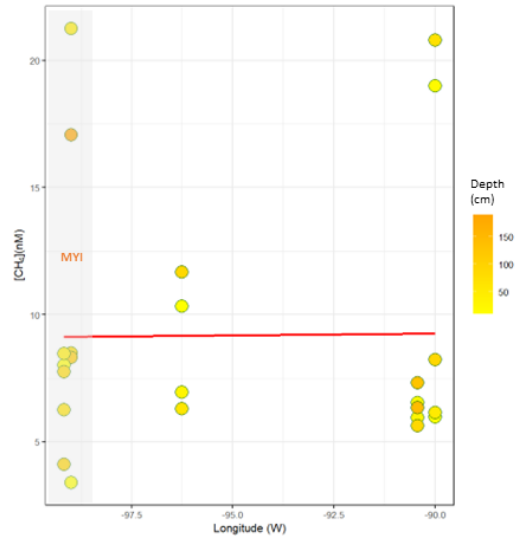
51



52

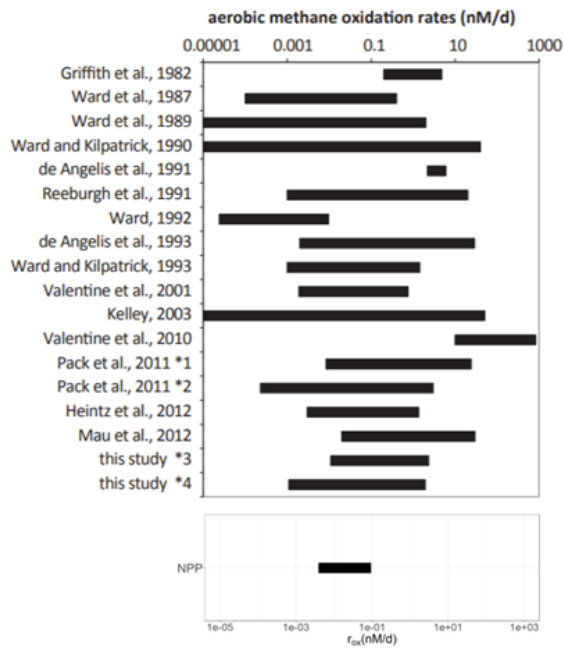
53 Figure S5: All methane vertical profiles within sea ice cores. In red are the in-situ $[CH_4]$, while in blue are
 54 the $[CH_4]$ at atmospheric equilibrium. The headers show the ice core numbers, as described in Fig.1.

55



56
 57 Figure S6: Methane concentrations within sea ice, across the longitudinal scale. The color code shows the
 58 sea ice core length (cm). The red line describes the linear model within the scattered data.

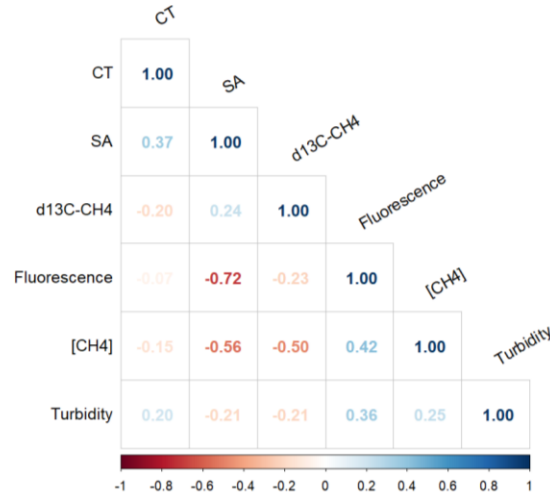
59



60
 61 Figure S7: comparison between methane oxidation rates measured in our study (NPP) and previous
 62 literature. The box on the top (from Mau et al., 2013) showed the range of methane oxidation rates measured
 63 at different locations in the ocean water column derived from tracer incubations using $^3\text{H-CH}_4$ (Reeburgh
 64 et al., 1991; Valentine et al., 2001, 2010; Heintz et al., 2012, Mau et al., 2012) or $^{14}\text{C-CH}_4$ (all others). Pack
 65 et al. (2011) compared incubations with $^3\text{H-CH}_4$ (*1) and incubations with low-level $^{14}\text{C-CH}_4$ (*2) that were
 66 measured with accelerator mass spectrometry. In this study, Mau et al. (2013) compared incubations with

67 $^3\text{H-CH}_4$ (*3) and incubations with $^{14}\text{C-CH}_4$ (*4). The box in the bottom showed the methane oxidation rates
 68 measured during the NPP expedition. The x axis is in log scale.

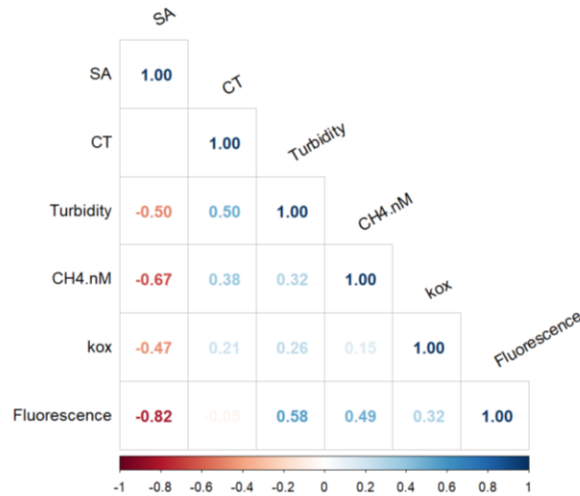
69



70

71 Figure S8: Spearman's correlation plot of in-situ methane data and physical data of the water masses.

72



73

74 Figure S9: Spearman's correlation plot of in-vitro methane oxidation rate and physical data of the water
 75 masses. Here, we also showed the in-situ methane concentration (CH4.nM) in order to relate it with the
 76 oxidation rate constant.

77